Continuous-Flow Reactor for Kinetic Analysis of Rapid Hydrothermal Reactions by Raman Spectroscopy

Yoshihiro Takebayashi,* Satoshi Yoda, Tsutomu Sugeta, and Katsuto Otake

National Institute of Advanced Industrial Science and Technology (AIST), Tsukuba, Ibaraki 305-8565, Japan
*E-mail: chikulin@ni.aist.go.jp

A high-temperature and high-pressure continuous-flow reactor combined with an in-situ Raman spectroscopic system has been developed for kinetic analysis of rapid hydrothermal reactions with half lives of several hundreds of ms to several ten seconds. The reactor was equipped with a new dead-volume-less optical cell with Λ-shaped flow path for a precise control of reaction time. The optical cell was designed for back-scattered Raman measurement and can be used up to 500 ºC and 30 MPa. A mixing method was utilized to quickly heat up aqueous sample solution to a reaction temperature. The homogeneity of the temperature in the reaction volume was realized by in-line temperature sensor units inserted into the flow line at the two positions, just after the mixing tee and just after the optical cell. To demonstrate the efficiency of the continuous-flow reactor, a kinetic study was carried out for hydrothermal decomposition of urea at 250-300 ºC and 27.5 MPa.

1. Introduction

High-temperature and high-pressure (HTHP) water has attracted increasing attention as a novel and environmentally benign medium for chemical reactions [1]. HTHP water can induce unique chemical reactions that do not occur in ambient water, and the reaction rate and pathway are strongly dependent on the temperature and pressure. To systematically control the hydrothermal reactions, a better understanding is needed of the reaction mechanism and kinetics in HTHP water. An in-situ spectroscopic monitoring combined with a mixing-flow reactor is a powerful tool for this purpose, especially for kinetic study of rapid hydrothermal reactions that complete in several seconds.

Raman spectroscopy has been widely used for in-situ monitoring of chemical reactions in HTHP water; e.g., decomposition of N_2H_4 [2], supercritical water oxidation of methane [3] and alcohols [4-6], and hydrolysis of acetonitrile [7]. Raman spectroscopy has several advantages over the complementary technique of IR spectroscopy in the design of optical cell for HTHP water; e.g., negligible background signal of solvent water and window materials. Most of the HTHP Raman cells reported, however, are inappropriate for the use of continuous-flow system for rapid hydrothermal reactions, because their large dead volume involved, especially around window sealing, brings about an ambiguity in the determination of the reaction time.

Both the reaction time and the reaction temperature should be carefully controlled in a kinetic analysis of reactions in HTHP water. A mixing method has been often used to shorten a heating time; a flow of aqueous sample solution is mixed with sufficiently preheated water to quickly start a hydrothermal reaction [8]. For a precise determination of the reaction time, no dead volume must be included in a flow line from the mixing to an in-situ optical detection. Furthermore, the temperature of the reaction volume must be kept at a desired reaction temperature. To attain the homogeneity of the temperature, it is necessary to monitor the temperature of the flowing aqueous solution at two or more positions in the reaction volume.

In the present work, we have developed a continuous-flow reactor equipped with a dead-volume-less Raman optical cell and with two in-line temperature sensors. The optical cell is designed for back-scattered Raman measurement, which requires only one window, simplifying the design of the cell. To eliminate a dead volume in the optical cell, a Λ-shaped flow path is employed. The in-line temperature sensor unit contains a sheathed thermocouple, which is directly inserted into a flowing fluid and can monitor the fluid temperature without disturbing the flow. Two

pieces of the sensor are inserted into the flow line to provide feedback to heating system. The details of the reactor are presented in the next section. We also report an experimental result carried out with this apparatus.

2. System Design and Operation

A schematic diagram of the whole system is shown in Fig. 1. The parts of the apparatus can be categorized into the three: a high-pressure continuous-flow reactor, an in-situ Raman monitoring system, and a temperature control system.

2.1. Continuous-Flow Reactor An aqueous sample solution is mixed with sufficiently hot water to quickly start hydrothermal reaction. Water and the aqueous solution are independently pressurized and pumped into the reactor with each syringe pump system. Each pump system consists of two syringe pumps (ISCO 100DM) which work alternately, i.e., one is pumping the fluid while the other is filling the syringe with the fluid, to provide a continuous fluid flow. The aqueous sample solution is directly introduced into a mixing tee, while the water in the other path is heated by a preheater (max. 1 kW) far above the reaction temperature. The hot water is then mixed with the aqueous sample solution, quickly heating up the sample to the reaction temperature. The mixing tee is made of Inconel 600, and the diameter of the flow path is 0.5 mm.

The reacting sample solution passes through a connecting tube made of Hastelloy C-276, and flows into a Raman optical cell. The size of the connecting tube is 1/16 inch in outer diameter and 0.5 mm in inner diameter. After the Raman measurement, the sample solution is cooled down, and finally goes out of the reactor via a back-pressure regulator (JASCO 880-81). The pressure inside the reactor is controlled within ± 0.1 MPa.

The reaction time t for the continuous-flow reactor is given by

$$t = V\rho / U . \tag{1}$$

The V is the inner volume of the reactor from the mixing point to the optical focus. The reaction volume can be varied by changing the length l of the connecting tube. Here we fixed the l at 384 mm, giving a reaction volume of 108 μL. The ρ is the density of the aqueous sample solution at the reaction temperature and pressure. In the following analysis, the density of the aqueous solution was
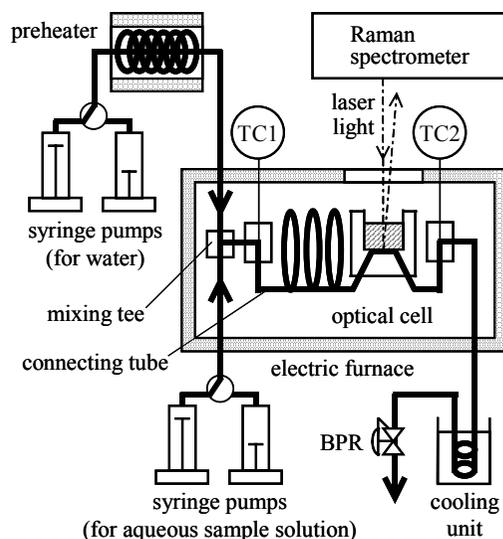

Fig. 1. Schematic diagram of our continuous-flow reactor. TC1 and TC2: thermocouples inserted into the temperature sensor units, BPR: back-pressure regulator.

approximated by the density of pure water; the latter is available in the literature [9]. The U is the total flow rate of both paths measured in ambient condition. The total flow rate was varied here from 0.1 to 25 mL/min with an accuracy of 0.3 %. This
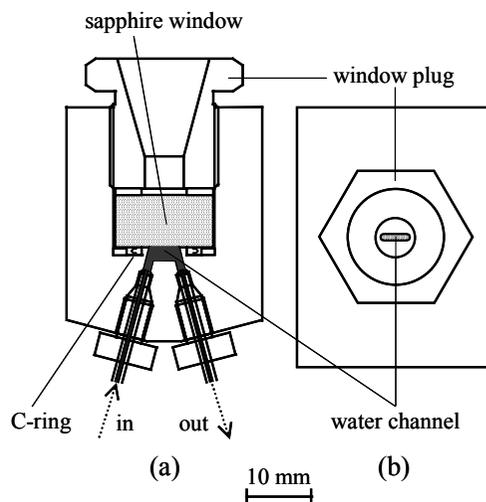

Fig. 2. High-temperature and high-pressure Raman optical cell. (a) Cross-section and (b) top view.

allows us to cover a range of reaction time t approximately from 0.2 to 50 s at 250-300 ˚C.

2.2. In-Situ Raman Monitoring System Figure 2 shows the HTHP Raman cell (Taiatsu Techno) designed for a combinational use with the continuous-flow reactor. The cell has a Λ-shaped flow path with negligible dead volume, and is equipped with a sapphire window (15 mm in diameter and 8 mm in thickness) for back-scattered Raman measurement. The aqueous sample solution introduced from the inlet on the bottom side goes up along a flow path (1 mm in diameter), passes through a flow channel (1 mm in width and 2 mm in depth) just under the window, and finally goes down to exit from the cell. The body of the cell is made of Hastelloy C-22, and the cell can be used at least up to 500 ºC and 30 MPa. The window is sealed by a gold-coated Inconel spring packing with C-shaped vertical cross-section [10]. The cell is rather simple, convenient for maintenance, and compact (45 mm in height, 30 mm in width, and 40 mm in depth). The inner volume of the cell is only 14 μL, the half of which (7 μL) is involved in the reaction volume. The extremely low volume makes ideal the kinetic analysis with the flow cell.

Raman measurements is made with an Ar^+ ion laser (NEC GLG-3280) tuned to 488 nm. The laser beam is focused into the optical cell at a power of 75 mW. The back-scattered light is led into a Raman spectrometer (JASCO NRS-1000), in front of which a holographic filter (Kaiser, Super Notch Plus) is placed. The light is dispersed by a grating (1200 lines/mm) and is detected with a CCD array (Princeton Instruments LN/CCD-2500PB) with a spectral resolution of 3 cm^{-1}.

2.3. Temperature Control System The reaction volume from the mixing tee to the optical cell is heated with a cylindrical electric furnace (Nikkato VT-620), in which a pyromax-DS heater (max. 1.0 kW) is embedded. The size of the furnace is 65 mm in inner diameter, 140 mm in outer diameter, and 250 mm in length. The furnace has a window for optical detection, and contains a cooling-water jacket to avoid heating of the optical system.

To monitor the temperature of the aqueous sample solution in the reaction volume, we have developed an in-line temperature sensor unit, as shown in Fig. 3. An Inconel-sheathed K-type thermocouple (Nimblox) is inserted directly into the fluid, not into the unit body, to measure the temperature of the flowing solution itself. The head
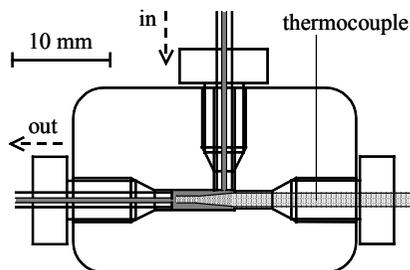

Fig. 3. Cross-section of temperature sensor unit.

of the thermocouple is tapered from 1.6 to 0.8 mm not to be in contact with the unit wall (2.0 mm in diameter). The temperature sensor units are inserted into the flow line at the two positions, immediately after the mixing tee (TC1 in Fig. 1) and immediately after the optical cell (TC2). The temperature monitored by TC1 provides feedback to the preheater, while the temperature monitored by TC2 to the electric furnace. The temperatures at TC1 and TC2 can be controlled within ± 1.0 ºC around the desired temperature.

3. Kinetic Analysis of Hydrothermal Decomposition of Urea

To test the performance of the system, a kinetic analysis has been made for a hydrothermal decomposition of urea at temperatures of 250-300 ºC and a constant pressure of 27.5 MPa. The reaction of urea has been studied by Brill et al. using an in-situ IR spectroscopy [11]. According to them, urea is rapidly decomposed into CO_2 and NH_3 through the two-step reaction via OCN^- as an intermediate:

$$(NH_2)_2CO \rightarrow OCN^- + NH_4^+ , \qquad (2)$$
$$OCN^- + NH_4^+ + H_2O \rightarrow CO_2 + 2NH_3 . \quad (3)$$
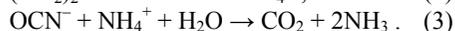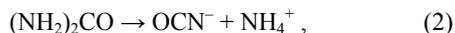
Here we aim to make a Raman spectroscopic detection of the reactant, intermediate, and product.

Urea (> 99 %) was used as purchased from Aldrich. Water was distilled and deionized to a specific resistance of 18 MΩ cm, and was deoxygenated by nitrogen. The aqueous urea solution was prepared at a concentration of 1.5 mol/L in ambient condition. The ratio of the flow rate of the sample solution to that of water was fixed at 2 : 3 in ambient condition. The Raman signals were collected for 30 s and were accumulated 10 times.
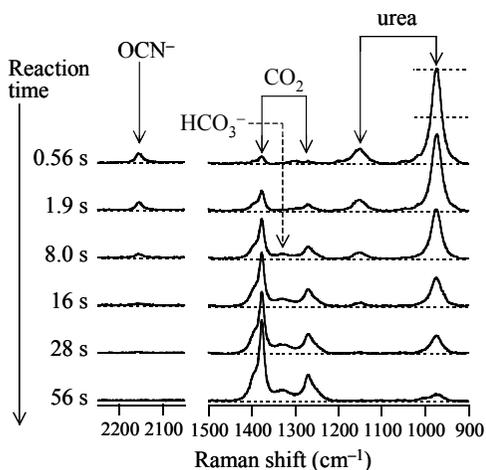
Fig. 4. Reaction time dependence of the Raman spectrum for the hydrothermal decomposition of urea at 250 ºC and 27.5 MPa.
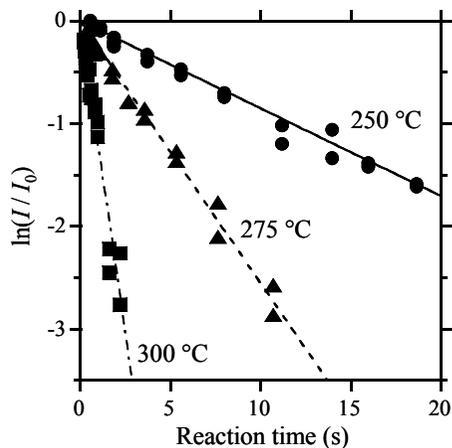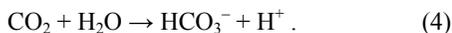

Fig. 5. Pseudo-first-order rate analysis for the hydrothermal decomposition of urea at 250, 275, and 300 ºC and 27.5 MPa. The I denotes the Raman intensity at 1150 cm^{-1} corresponding to urea.

Figure 4 shows typical Raman spectra at different reaction times at 250 ºC and 27.5 MPa. It is evident that the peaks at 1150 and 972 cm^{-1}, corresponding to the urea's ν_3 and ν_4 vibrational modes [12], decrease with the reaction time. At reaction times longer than 28 s, the peak at 1150 cm^{-1} is hardly observed. The Raman intensity at 972 cm^{-1}, however, never decays to zero, because the ν_4 signal is overlapped with a signal of HCO$_3^-$. Thus, in the kinetic analysis described later, the concentration of urea was determined from the signal intensity at 1150 cm^{-1}.

A closer look reveals another decaying signal at 2156 cm^{-1}. The small peak is ascribed to the ν_{CN} band of OCN$^-$ [13]. The OCN$^-$ signal also disappears in 28 s. We can find, on the other hand, rising signals at 1381 and 1273 cm^{-1}. The two peaks are assigned to the Fermi dyads of CO$_2$ [14], resulting from the resonance of the symmetric stretching mode ν_1 and the overtone of the bending mode $2\nu_2$. The species detected above are consistent with Eqs. (2) and (3).

At reaction times longer than 8 s, a new peak appears between the dyads of CO$_2$. The new peak at 1328 cm^{-1} is ascribed to the ν_3 band of HCO$_3^-$ [15]. The in-situ detection of HCO$_3^-$ shows that in HTHP water at 250 ºC, a CO$_2$ molecule considerably dissociates as

$$CO_2 + H_2O \rightarrow HCO_3^- + H^+ . \qquad (4)$$

At temperatures higher than 300 ºC, however, the HCO$_3^-$ signal was hardly detected, indicating that the dissociation to the ionic form is less favored at higher temperatures under the isobaric conditions.

We further determined the rate constant k for the reaction (2) at temperatures of 250, 275, and 300 ºC. Figure 5 shows the reaction time dependence of the intensity of the urea signal at 1150 cm^{-1}. The time profile can be interpreted in terms of a pseudo-first-order kinetics. The rate constant thus obtained is 0.089 ± 0.003 s^{-1} at 250 ºC, 0.30 ± 0.02 s^{-1} at 275 ºC, and 1.19 ± 0.09 s^{-1} at 300 ºC, yielding the activation energy of 129 ± 8 kJ/mol. The rate constant obtained here differs a little from that reported by Brill et al. (0.14 s^{-1} at 250 ºC, 0.33 s^{-1} at 275 ºC, and 0.97 s^{-1} at 300 ºC) [11]; the activation energy of their result (84 kJ/mol) is much smaller than that of ours. A possible reason for the difference is that no mixing-flow system is employed in their apparatus; a sample solution is heated only by the cell body, leading to an ambiguity of the reaction time and temperature.

4. Conclusions

Our continuous-flow reactor newly designed for an in-situ Raman monitoring of rapid hydrothermal reactions has several features in precisely controlling the reaction time and the reaction temperature. The reactor was applied to a kinetic

analysis of hydrothermal decomposition of urea at 250-300 ºC and 27.5 MPa, where the half life of urea was found to be in the range of 7.8 to 0.58 s. We are currently improving the apparatus to study the reactions with shorter half lives and those at higher temperatures including supercritical conditions.

References and Notes

[1] See, e.g., (a) P. E. Savage, *Chem. Rev.*, **99**, 603 (1999); (b) D. Bröll, C. Kaul, A. Krämer, P. Krammer, T. Richter, M. Jung, H. Vogel, and P. Zehner, *Angew. Chem. Int. Ed.*, **38**, 2998 (1999); J. An, L. Bagnell, T. Cablewski, C. R. Strauss, and R. W. Trainor, *J. Org. Chem.*, **62**, 2505 (1997); and references cited therein.

[2] D. A. Masten, B. R. Foy, D. M. Harradine, and R. B. Dyer, *J. Phys. Chem.*, **97**, 8557 (1993).

[3] R. R. Steeper, S. F. Rice, I. M. Kennedy, and J. D. Aiken, *J. Phys. Chem.*, **100**, 184 (1996).

[4] S. F. Rice, T. B. Hunter, Å. C. Rydén, and R. G. Hanush, *Ind. Eng. Chem. Res.*, **35**, 2161 (1996).

[5] T. B. Hunter, S. F. Rice, and R. G. Hanush, *Ind. Eng. Chem. Res.*, **35**, 3984 (1996).

[6] S. Koda, N. Kanno, and H. Fujiwara, *Ind. Eng. Chem. Res.*, **40**, 3861 (2001).

[7] E. Venardou, E. Garcia-Verdugo, S. J. Barlow, Y. E. Gorbaty, and M. Poliakoff, *Vib. Spectrosc.*, **35**, 103 (2004).

[8] See, e.g., F. Amita, H. Oka, M. Mukaide, Y. Urasaki, K. Takegoshi, T. Terao, and O. Kajimoto, *Rev. Sci. Instrum.*, **75**, 467 (2004).

[9] S. A. Klein, and A. H. Harvey, *NIST/ASME Steam Properties*, *NIST Standard Reference Database 10* (1996)

[10] Taiatsu Techno, *Japan Patent*, 2000-136996.

[11] M. L. Kieke, J. W. Schoppelrei, and T. B. Brill, *J. Phys. Chem.*, **100**, 7455 (1996).

[12] A. Yamaguchi, T. Miyazawa, T. Shimanouchi, and S. Mizushima, *Spectrochim. Acta*, **10**, 170 (1957).

[13] P. W. Schultz, G. E. Leroi, and A. L. Popov, *J. Amer. Chem. Soc.*, **117**, 10735 (1995).

[14] M. S. Brown and R. R. Steeper, *Appl. Spectrosc.*, **45**, 1733 (1991).

[15] A. R. Davis and B. G. Oliver, *J. Sol. Chem.*, **1**, 329 (1972).